ACS APPLIED MATERIALS & INTERFACES

Research Article

www.acsami.org

Mesoporous SnO_2-Coated Metal Nanoparticles with Enhanced Catalytic Efficiency

Na Zhou,[†,‡] Lakshminarayana Polavarapu,[†] Qing Wang,[‡,§] and Qing-Hua Xu*[,†,‡]

[†]Department of Chemistry, National University of Singapore, Singapore 117543

[‡]NUSNNI-Nanocore, National University of Singapore, Singapore 117576

[§]Department of Materials Science and Engineering, National University of Singapore, Singapore 117576

Supporting Information

ABSTRACT: Aggregation of plasmonic nanoparticles under harsh conditions has been one of the major obstacles to their potential applications. Here we present the preparation of uniform mesoporous SnO_2 shell coated Au nanospheres, Au nanorods and Au/Ag core−shell nanorods and their applications in molecular sensing and catalysis. In these nanostructures, the mesoporous SnO_2 shell stabilizes the metal nanoparticle and allows the metal core to be exposed to the surrounding environment for various applications at the same time. These nanostructures display high refractive index sensitivity, which makes them promising materials for LSPR based molecular sensing. Applications of these materials as catalysts for reduction of 4-nitrophenol by $NaBH_4$ have also been demonstrated. Both uncoated and SnO_2-coated anisotropic Au and Au/Ag nanorods were found to display significantly better catalytic efficiency compared to the corresponding spherical Au nanoparticles. Catalytic activities of different metal nanoparticles were significantly enhanced by 4−6 times upon coating with the mesoporous SnO_2 shell. The enhanced catalytic activity of metal nanoparticles upon SnO_2 coating was attributed to charge-redistribution between noble metal and SnO_2 that disperses the electrons to a large area and prolonged electron lifetime in SnO_2-coated metal nanoparticles. The charge transfer mechanism of enhanced catalytic efficiency for SnO_2-coated metal nanoparticles has been further demonstrated by photochemical reduction of silver ions on the outer surface of these NPs. These metal/semiconductor core−shell nanomaterials are potentially useful for various applications such as molecular sensing and catalysis.

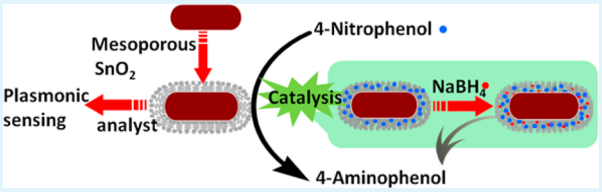

KEYWORDS: *mesoporous SnO_2, metal nanoparticle, core−shell structure, plasmon resonance, sensing, catalysis*

INTRODUCTION

Noble metal nanoparticles (NPs) have received great attention because of their interesting properties and potential applications in photonics, electronics, sensing and catalysis.[1−3] They display unique optical properties known as localized surface plasmon resonance (LSPR). LSPR band is not only strongly dependent on the morphology of the nanoparticles themselves,[4,5] but also sensitive to the refractive index of the surface bound molecules and surrounding environments. Strong dependence of the LSPR band on local environment has been utilized to develop LSPR based molecular sensing.[6] Noble metal NPs have also been known to act as catalysts for various organic reactions.[7] However, noble metal NPs generally suffer from poor stability and tend to form aggregates in harsh environments,[8,9] which hampers their various practical applications.[10] Formation of metal NPs aggregate will induce a large shift in the LSPR band, which interferes with their applications in LSPR based sensing.[11,12] A lot of efforts have been devoted to stabilize metal NPs by immobilizing them on supports such as metal oxides,[13−15] silica,[16] carbon nanotube,[17] or polymeric materials.[18] SiO_2, TiO_2, and polymer-coated metal NPs have recently attracted lots of attention because these coating shells can not only stabilize metal NPs, but also introduce new functionalities to exhibit unique multifunctional advantages.[19,20]

One important requirement for the coating shell is permeability to allow external molecules or reactants to diffuse into direct contact and interact with the metal core. Mesoporous shells are attractive coating materials as they are permeable to small molecules to maintain catalytic properties of the metal core. Mesoporous SiO_2-coated metal NPs are of particular interest because of their easy preparation.[21,22] SiO_2 shell can improve their biocompatibility and allow modification with other molecules to display multifunctional capability.[19,20] However, mesoporous silica-coated NPs also suffer from long-term stability in water and tend to aggregate at slightly basic conditions, which limit their applications.[23] It is highly desirable to search for new coating materials to develop more efficient, durable, and eco-friendly catalysts.

Mesoporous SnO_2-coated spherical Au nanospheres were successfully prepared by Oldfield et al.[24] Application of SnO_2 coated Au nanospheres as catalyst for CO oxidation was

Received: December 13, 2014
Accepted: February 12, 2015
Published: February 12, 2015

DOI: 10.1021/am508803c
ACS Appl. Mater. Interfaces 2015, 7, 4844−4850

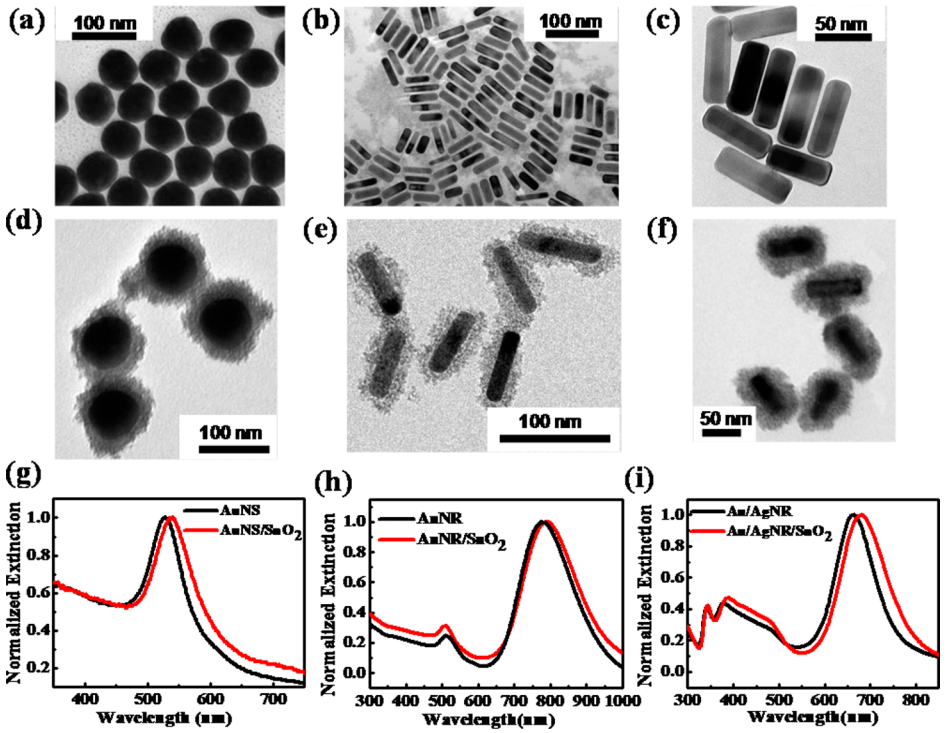

Figure 1. TEM images of (a) AuNS, (b) AuNR, (c) Au/AgNR, (d) AuNS/SnO_2, (e) AuNR/SnO_2, (f) Au/AgNR/SnO_2. Their corresponding UV–vis extinction spectra are shown in g–i.

subsequently explored by Yu et al.[25] A very recent report by Lee et al. showed that SnO_2 coated gold nanospheres displayed better stability than SiO_2 coated ones at basic conditions.[26] So far most of the studies focus on SnO_2 coated nanospheres. Anisotropic nanostructures such as nanorods have been known to display more profound optical properties.[27,28] Mesoporous SnO_2 coated anisotropic metal nanostructures are expected to display interesting multifunctional capability for various potential applications, which have not been explored so far.

Here we report a series of mesoporous SnO_2 coated noble metal NPs such as Au nanospheres (NSs), Au nanorods (NRs) and core–shell Au/AgNRs. SnO_2 shell was coated onto metal NPs by a simple one-pot hydrothermal reaction. SnO_2 shell helps to protect the metal NPs from aggregation in harsh environments, which significantly improves their stability. These SnO_2-coated metal NPs exhibited significant redshift in LSPR as the refractive index of the medium increased, confirming the mesoporous nature of the SnO_2 shell, which allows external molecules to access metal core for various applications. High refractive index sensitivity of Au/AgNR/SnO_2 makes them promising materials for LSPR based molecular sensing. Applications of these materials as catalysts have been demonstrated in the reduction reaction of 4-nitrophenol by $NaBH_4$. Both uncoated and SnO_2-coated anisotropic Au NR and Au/Ag NR displayed much better catalytic activities than the corresponding spherical Au nanoparticles. Catalytic activities of different metal NPs were significantly enhanced upon coating with mesoporous SnO_2 shell. The charge transfer mechanism of enhanced catalytic efficiency of coated metal nanoparticles has been proposed and demonstrated by photochemical reduction of silver ions on the surface of these nanoparticles.

EXPERIMENTAL SECTION

Materials. Hexadecyltrimethylammonium bromide (CTAB, 98%), cetyltrimethylammonium chloride solution (CTAC, 25%), sodium borohydride ($NaBH_4$, 99%), gold(III) chloride trihydrate ($HAuCl_4 \cdot 3H_2O$, 99.9%) and sodium stannate trihydrate ($Na_2SnO_3 \cdot 3H_2O$, 95%) were purchased from Sigma-Aldrich. Silver nitrate ($AgNO_3$), L-(+)-ascorbic acid, and 4-nitrophenol were purchased from Alfa Aesar. Deionized (DI) water was used in all the experiments.

Instruments. UV–vis extinction spectra were measured by using a Shimadzu UV 2550 spectrometer. Reduction of 4-nitrophenol by $NaBH_4$ was monitored by using an Agilent diode-array UV–vis spectrophotometer, which can measure one spectrum within 1 s. Transmission electron microscopy (TEM) images were taken on a JEOL 1220 electron microscope. High-resolution TEM images were taken on a Philips EM300 electron microscope operated at an accelerating voltage of 300 kV. X-ray diffraction (XRD) patterns were collected using a Bruker GADDS D8 Discover diffractometer with Cu_{Ka} radiation (1.5418 Å).

Preparation of SnO_2-Coated Au and Au/Ag NPs. AuNSs, AuNRs and Au/AgNRs were prepared by using previously reported methods.[28−31] The details are described in the Supporting Information. AuNS/SnO_2 was prepared by following the method previously reported by Oldfield et al.[24] We extended this method to the preparation of AuNR/SnO_2 and Au/AgNR/SnO_2. Briefly, 5.0 mL of CTAB capped AuNRs were diluted to 20.0 mL with DI water in a round-bottom flask. The pH of the solution was adjusted to 10.5 by addition of NaOH. The solution was kept inside a 75 °C oil bath under vigorous stirring for 15 min, followed by rapid addition of 3.0 mL of freshly prepared Na_2SnO_3 aqueous solution (0.004M). After stirring for another 2 h, the obtained AuNR/SnO_2 NPs were centrifuged at 7000 rpm, washed twice and redispersed in 5.0 mL of DI water. SnO_2-coated Au/AgNR were prepared by using 4.0 mL of Au/AgNR and 2.0 mL of 0.004 M Na_2SnO_3.

Catalyzed Reduction of 4-Nitrophenol. Two-hundred microliters of AuNR and AuNR/SnO_2 (or 330 μL of AuNS and AuNS/SnO_2, or 100 μL of Au/AgNR and Au/AgNR/SnO_2 so that catalytic efficiency of these NPs are compared on the base of containing same mass of Au or Au/Ag core) were homogeneously dispersed into 2.0

DOI: 10.1021/am508803c
ACS Appl. Mater. Interfaces 2015, 7, 4844–4850

mL of 4-nitrophenol aqueous solution (10.0 mg/L) in a quartz cuvette followed by rapid injection of 20.0 μL of freshly prepared $NaBH_4$ (10.0 g/L). The initial molar ratio of 4-nitrophenol and $NaBH_4$ were kept at 1:36 in all the experiments. The amount of $NaBH_4$ is excessive for reduction of 4-nitrophenol so that the concentration of $NaBH_4$ could be considered as nearly constant in the whole reaction process. The extinction spectra were measured at regular intervals. All the reactions were performed at 298 K.

Photochemical Reduction of Ag^+ on the Surface of AuNR/SnO_2. One-half a milliliter of AuNR/SnO_2 NPs dispersion was diluted to 2 mL with DI water in a quart cuvette before 30 μL of 0.01 M $AgNO_3$ were added. The mixture solution was purged with N_2 gas for 5 min to remove the inside O_2 before the cuvette was sealed. The solution was then irradiated with a 775 nm laser beam (50 mW) for 35 min.

RESULTS AND DISCUSSION

Figure 1 shows TEM images and extinction spectra of the prepared AuNSs, AuNRs and Au/AgNRs before and after coating with SnO_2. The prepared AuNSs have an average diameter of 62 nm with LSPR band maximum at 531 nm. The LSPR band maximum was found to redshift to 538 nm after coating with 15 nm thick SnO_2 shells (size distributions of Au NS core diameters and SnO_2 shell thickness are shown in Figure S1a in the Supporting Information), which can be ascribed to an overall increase in the refractive index of the dielectric environment surrounding AuNSs.[24,32] The same method was extended to prepare SnO_2 coated AuNRs and Au/AgNRs. The average diameter and length of Au NRs are 18 and 63 nm (The size distribution was summarized in Figure S1b in the Supporting Information). The extinction spectrum of the Au NRs dispersion displays a transverse LSPR band at 509 nm and a longitudinal LSPR band at 774 nm, respectively. The longitudinal LSPR band of AuNRs was found to redshift to 790 nm upon coating with 15 nm thick SnO_2 shells. Au/AgNRs were prepared by coating the 18 × 63 nm AuNRs with 5.1 nm thick layer of Ag. The longitudinal LSPR band of Au/AgNRs at 662 nm was found to redshift to 680 nm after coating with 15 nm-thick SnO_2 shells (The distribution of SnO_2 shell thickness was summarized in Figure S1c in the Supporting Information). The redshift of longitudinal LSPR band of AuNRs and Au/AgNRs can also be ascribed to increasing refractive index of the surrounding dielectric environment. AuNS/SnO_2, AuNR/SnO_2, and Au/AgNR/SnO_2 NPs have also been characterized with X-ray diffraction (XRD) pattern and high-resolution TEM image (see Figure S2 in the Supporting Information). The lattice fringes obtained from HR-TEM matched well with the planes of SnO_2 obtained from XRD data.

TEM images of AuNS/SnO_2, AuNR/SnO_2, and Au/AgNR/SnO_2 (Figure 1d–f) indicated that the outer SnO_2 shells are mesoporous. The mesoporous structure of the SnO_2 shell allows exposure of the noble metal core to the surrounding environment to maintain their catalytic properties while improving the stability of NPs in various organic solvents. CTAB-capped Au NRs were known to form aggregates in organic solvents,[8,9] which was confirmed in our experiments (Figure S3 in the Supporting Information). SnO_2-coated Au NRs were found to disperse very well in water and various organic solvents such as ethanol, DMF, and DMSO, as evidenced in the photograph and extinction spectra shown in Figure S3 in the Supporting Information. These SnO_2-coated NPs were also quite stable in aqueous solution of different pH, even very basic solutions (see Figure S3c in the Supporting Information). The high stability of metal/SnO_2 NPs in different harsh environments is beneficial for their potential applications. The mesoporous nature of the SnO_2 shell was confirmed by measuring extinction spectra of these core–shell NPs in water–DMF mixture solvents with varying volume ratios to change their refractive index. The longitudinal LSPR band of AuNR/SnO_2 was found to steadily redshift as the refractive index of the mixture solvent increased (Figure 2b). Similar redshift in

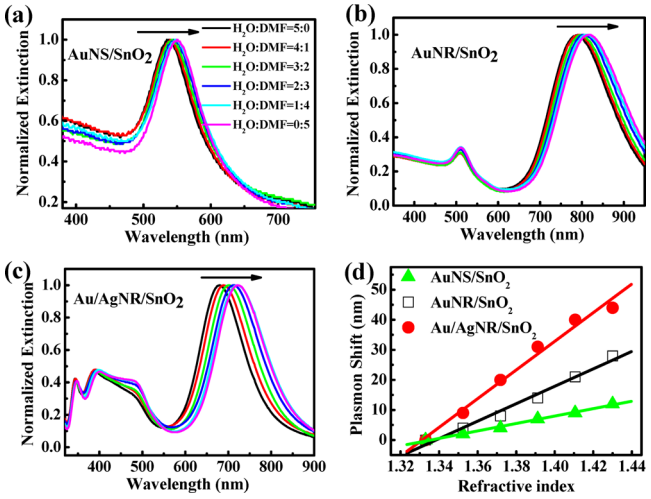

Figure 2. Normalized extinction spectra of (a) AuNS/SnO_2, (b) AuNR/SnO_2 and (c) Au/AgNR/SnO_2 in water-DMF liquid mixture solvent of varying volume ratios. (d) LSPR band shift of AuNS/SnO_2, AuNR/SnO_2 ,and Au/Ag/SnO_2 versus refractive index of the medium.

LSPR band was observed for AuNS/SnO_2 and Au/AgNR/SnO_2 (Figures 2a, c), which confirms that the mesoporous structure of the SnO_2 shells allows exposure of the metal cores to the surrounding environments. The linear regression analysis of the redshift in LSPR band yielded a refractive index sensitivity of 124 nm/RIU (refractive index unit) for AuNS/SnO_2, 290 nm/RIU for AuNR/SnO_2, and 477 nm/RIU for Au/AgNR/SnO_2, respectively. AgNPs have been known to display larger refractive index sensitivity than AuNPs of the same shape.[33,34] On the other hand, rod-shape NPs display larger refractive index sensitivity than spherical NPs.[35,36] AgNRs are expected to display exceptional refractive index sensitivity. However, AgNRs have been known to be very unstable.[37] Au/AgNRs have been proposed as the alternative for LSPR-based molecular sensing with exceptional sensitivity.[33] In combination with their improved stability by SnO_2 coating, high refractive index sensitivity of our Au/AgNR/SnO_2 makes them promising materials for LSPR-based molecular sensing.

Catalytic efficiency of these metal NPs was tested by catalytic reduction of nitrophenol to aminophenol. Aminophenol is an important intermediate for medicines, dyes, and organic synthesis.[33,34] The reduction rate of nitrophenol to aminophenol by $NaBH_4$ in the absence of catalyst is very slow.[38] Noble metal NPs have been demonstrated to display good catalytic activity for reduction reaction of nitrophenol.[7,36] Figure 3 showed catalytic activities of AuNS/SnO_2, AuNR/SnO_2 and Au/AgNR/SnO_2 for reduction of 4-nitrophenol to 4-aminophenol. The progress of the reduction reaction was monitored through their UV–vis absorption spectra (Figures 3a and Figure S4 in the Supporting Information). 4-Nitrophenol in water has an absorption band around 317 nm (Figure S4 in the Supporting Information).[39] Addition of $NaBH_4$ resulted in immediate formation of 4-nitrophenolate

DOI: 10.1021/am508803c
ACS Appl. Mater. Interfaces 2015, 7, 4844–4850

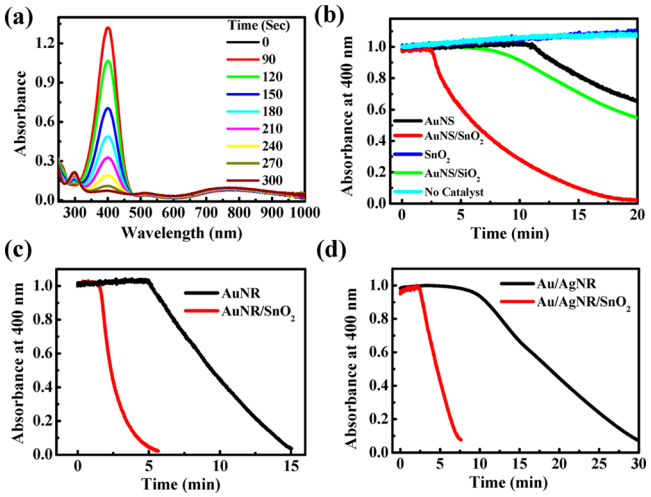

Figure 3. (a) Evolution of UV−vis absorption spectra during the course of reduction of 4-nitrophenolate by $NaBH_4$ using AuNR/SnO_2 as the catalyst. (b−d) Normalized absorbance (normalized against the initial point) at 400 nm as a function of time in the absence and presence of different NPs as the catalyst: (b) AuNS and AuNS/SnO_2; (c) AuNR and AuNR/SnO_2; (d) Au/AgNR and Au/AgNR/SnO_2. The results of using SnO_2 and AuNS/SiO_2 as catalyst are shown in b for direct comparison.

ions, which displayed an absorption band around 400 nm (Figure S4 in the Supporting Information).[10,39] The final product 4-aminephenol has an absorption band around 297 nm.[10,39] Figure 3a shows the evolution of UV−vis spectra of the reaction mixture after adding $NaBH_4$ into the mixture of 4-nitrophenol and the AuNR/SnO_2 catalyst. It can be clearly seen that a gradual decrease in absorption band around 400 nm is accompanied by simultaneous increase in absorption around 297 nm, indicating gradual conversion of 4-nitrophenolate into 4-aminophenol.[40] The observation of two isosbestic points at 277 and 317 nm indicates that conversion of 4-nitrophenolate into 4-aminophenol occurred without any side reactions.[27,35] Catalysis kinetics of these reactions were examined by monitoring the change in absorbance at 400 nm during the course of reduction reaction (Figure 3). It can be seen that reduction reaction did not take place in the absence of any catalyst or in the presence of SnO_2 NPs (Figure 3b). In the presence of various uncoated and coated metal NPs acting as the catalyst, the reaction took places after an induction period, during which $NaBH_4$ reacts with the dissolved oxygen and became adsorbed onto the surface of catalysts.[40] When AuNR was used as the catalyst, the induction time is 320 s and it took another 240 s to reduce 50% of 4-nitrophenolate. When SnO_2-coated AuNR was used at the catalyst, not only the induction period was shortened, the reduction reaction rate also became much faster. The induction time became ∼90 s and it only took another 47 s to reduce ∼50% of 4-nitrophenolate when AuNR/SnO_2 was used as the catalyst. The rate constant of catalytic reduction reactions can be estimated by using the Langmuir−Hinshelwood apparent first-order kinetics model to fit the $\ln(C/C_0)-t$ data (Figure S5 in the Supporting Information), where C_0 and C are initial and time-dependent concentration of 4-nitrophenolate ions.[41] The fitting results are summarized in Table 1. The rate of AuNR/SnO_2 catalyzed reaction was found to be ∼5.0 times faster than that of AuNR catalyzed reaction. We have also tested the catalytic activity of AuNR/SnO_2 with a different shell thickness of 10 nm (Figure S6 in the Supporting Information). AuNR/SnO_2-10 nm was found to display slightly lower catalytic efficiency compared to that of AuNR/SnO_2-15 nm.

Table 1. Summary of Induction Time and Rate Constants for Different Catalysts

catalysts		induction time (min)	rate constant (min^{-1})
AuNS	uncoated metal	11.20	0.04
	SnO_2 coated	2.25	0.18
	SiO_2 coated	8.18	0.046
AuNR	uncoated metal	5.33	0.18
	SnO_2 coated	1.50	0.90
Au/AgNR	uncoated metal	9.93	0.08
	SnO_2 coated	2.40	0.50

We have also tested the catalytic property of AuNS/SnO_2 and Au/AgNR/SnO_2 in comparison with uncoated AuNS and Au/AgNR, respectively (Figure 3b, d). The induction times and rate constants for different catalysts are summarized in Table 1. Among all the uncoated metal NPs, AuNS and Au/AgNR showed lower catalytic efficiency compared to AuNR. The reaction rate constants increase in the order of AuNS < Au/AgNR < AuNR. Similar to the results of AuNR, the catalytic activities of AuNS and Ag/AgNR have also been significantly enhanced (by 4−6 folds) upon coating with the mesoporous SnO_2 shell.

The different catalytic activities of AuNSs, Au/AgNRs, and AuNRs can be partially ascribed to their different surface areas as the measurements were conducted by using materials containing noble metals of the same mass. As the volume of Au NSs is larger than Au NRs, the number of Au NSs is less than that of Au NRs. Consequently, the surface area of AuNSs is less than that of Au NRs and the catalytic efficiency of Au NSs with the same mass is lower than Au NRs. In addition to the similar volume effects, the interactions between Au and Ag are also responsible for lower catalytic activity of Au/AgNRs compared to AuNRs. In the Au/Ag core−shell structure, Au and Ag intimately contact with each other. Electron equilibration from Ag to Au will cause some electrons transfer to the inner Au core,[42,43] which are not accessible by the reactant and result in reduced catalytic ability.

AuNS/SiO_2 has been previously reported to act as the catalyst for reduction of 4-nitrophenolate, which displayed reduced catalytic activity compared to uncoated AuNS. The catalytic properties could be improved by etching the noble metal core to create a cavity between AuNS and SiO_2.[21] TiO_2-coated AuNPs have also been previously reported to stabilize the catalytic AuNPs. However, its catalytic efficiency was also lower than that of uncoated AuNPs.[15,44] We have also prepared mesoporous SnO_2 coated AuNS and compared its catalytic activity with AuNS and SiO_2 coated AuNS (TEM images of AuNS/SiO_2 are shown in Figure S7 in the Supporting Information). When AuNS/SiO_2 was used as the catalyst, the reduction rate constant was found to be similar to that when AuNS was used as the catalyst, although the induction time was slightly shortened (Figure 3b). When AuNS/SnO_2 was used as the catalyst, not only the induction time was shortened, the reduction rate has been significantly increased (Figure 3b and Table 1). These results demonstrate that mesoporous SiO_2 or SnO_2 shell is permeable to allow 4-nitrophenol molecules come into direct contact with the Au NP surface to maintain its catalytic activity. The fact that mesoporous SnO_2-coated Au

DOI: 10.1021/am508803c
ACS Appl. Mater. Interfaces 2015, 7, 4844−4850

NPs shows better catalytic activity than mesoporous SiO_2 coated Au NPs indicating that the enhanced catalytic efficiency of SnO_2 coated metal NPs is due to the intrinsic properties of SnO_2.

Different catalytic behaviors for SiO_2-, TiO_2-, and SnO_2-coated metal NPs could be understood by the mechanism as illustrated in Scheme 1. When noble metal NPs act as the catalyst for reduction of 4-nitrophenol by $NaBH_4$, electrons from BH_4^- were transferred to noble metal NPs first and then subsequently transferred to the 4-nitrophenol molecules adsorbed on the surface of the noble metal to reduce 4-nitrophenol. When SiO_2, TiO_2 or SnO_2 coated metal NPs were used as the catalyst, BH_4^- ions can travel through the mesoporous coating shell and come into direct contact with the metal surface to transfer the electrons to metal NPs. The electrons were subsequently captured by the adsorbed 4-nitrophenol (Scheme 1a). Better catalytic efficiency of SnO_2-coated metal NPs could be ascribed to a synergistic effect between SnO_2 and plasmonic metal.[45] When metal and semiconductors are placed in contact, Fermi level alignment will result in charge redistribution: electrons will leave the metal into the semiconductor. When metal/SnO_2 NPs were used as the catalyst, electrons injected by BH_4^- to the metal surface can transfer to SnO_2. Mesoporous SnO_2 helps metal NPs disperse electrons to a large area and increase the chances for 4-nitrophenol to capture the electrons to be reduced, so as to enhance the catalytic activity. There is no such charge redistribution between SiO_2 and Au in Au/SiO_2 NPs due to the insulator nature of SiO_2. Charge redistribution will occur between Au and TiO_2 in Au/TiO_2 nanostructures, in which electrons transferred from Au to the conduction band of TiO_2 will reduce 4-nitrophenol.[46] However, these electrons can also be captured by H_2O as the conduction band of TiO_2 is higher than that required for reduction of H^+/H_2O to H_2 (Scheme 1b).[47] AuNS/TiO_2 has been previously demonstrated to act as photocatalyst for water splitting to generate H_2 under visible-light irradiation.[48] Competition between reduction of 4-nitrophenol and H_2O thus decreases the reaction rate of 4-nitrophenol reduction. However, the conduction band of SnO_2 is lower than that required for reduction of H^+ (Scheme 1c). The electrons on the conduction band of SnO_2 can only be captured by 4-nitrophenol without the competition reaction with H^+/H_2O.

Scheme 1. Proposed Mechanisms to Illustrate (a) Enhanced Catalytic Activities in Mesoporous SnO_2-Coated Metal NPs, and (b, c) Different Catalytic Activities of SnO_2- and TiO_2-Coated Metal NPs Due to Competing Reduction of H_2O by Au/TiO_2

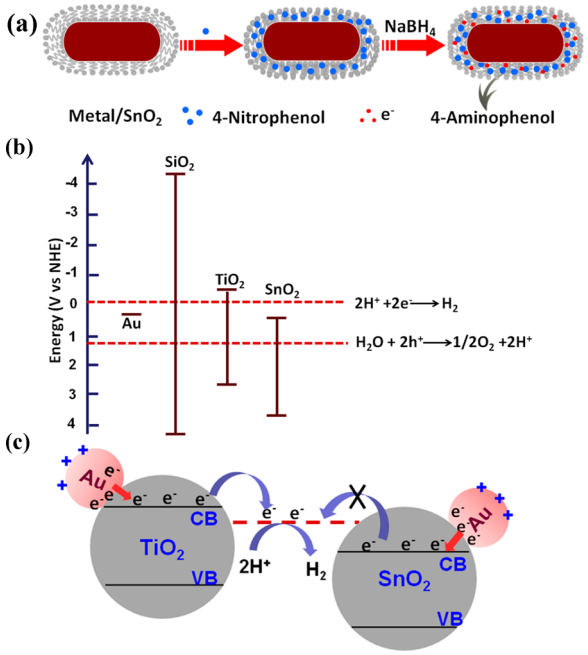

In a recent study on catalytic properties of Ag-carbon nanofibers hybrid nanomaterials,[38] Zhang et al. proposed that electrons in the semiconductor can increases the chances of reducing absorbed 4-nitrophenol, which is consistent with our observation here. In another study on AuNS/SnO_2, Oldfield et al. observed that the capacitance of Au NSs will increase upon coating with SnO_2.[24] This suggests the lifetime of electrons on the metal NPs will be prolonged, which will also promote the interactions between the electrons and 4-nitrophenol. Consequently, SnO_2 coating shells will help to improve catalytic activity of various noble metal NPs.

To further confirm the above proposed charge transfer mechanism for enhanced catalytic efficiency of SnO_2-coated metal NPs, we have designed a photochemical reduction of Ag^+ ions on the surface of AuNR/SnO_2 (Figure 4). A cuvette containing $AgNO_3$ and AuNR/SnO_2 NPs was illuminated with a 775 nm laser beam for 35 min. Additional Ag NPs was found to form on the outer surface of Au NR/SnO_2 NPs, which can be clearly observed from the TEM images (Figure 4a). The formation Ag NPs was also confirmed by comparing the extinction spectra before and after laser irradiation (Figure 4b), where a clear increase of extinction in the wavelength range of

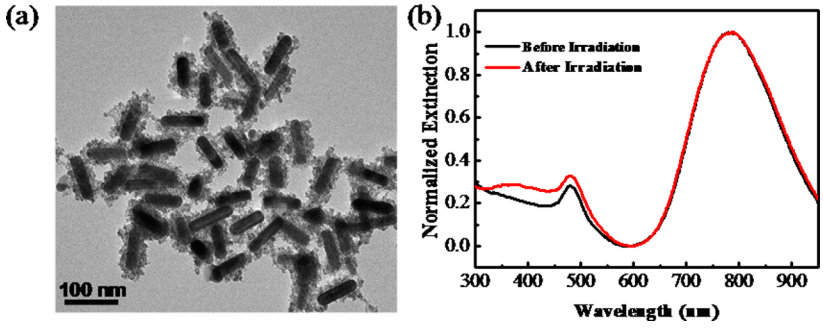

Figure 4. (a) TEM images and (b) UV–vis extinction spectra of AuNR/SnO_2 NPs and $AgNO_3$ mixture solution after irradiation with a 775 nm laser beam for 35 min. Extinction spectra of AuNR/SnO_2 NPs before laser irradiation were plotted in b for direct comparison.

DOI: 10.1021/am508803c
ACS Appl. Mater. Interfaces 2015, 7, 4844–4850

350−550 nm due to formation of additional Ag NPs was observed. As 775 nm can only excite Au NRs, not SnO_2, hot electrons will be injected from Au to SnO_2. These electrons were subsequently captured by Ag^+ ions to reduce them to Ag NPs on the surface of SnO_2. The observations in Figure 4 unambiguously confirm the charge transfer process from Au NRs to SnO_2. These electrons on the surface of SnO_2 could subsequently be utilized to reduce $AgNO_3$ or 4-nitrophenol.

We have also tested the recyclability of these NPs and the results are summarized in Table S1 in the Supporting Information. It was found that there was a noticeable reduction in their catalytic activity after the second cycle of use. We have checked the TEM images of these metal/SnO_2 NPs before and after catalytic reactions (Figure S8 in the Supporting Information). No change in the size and shell thickness of the NPs was observed, indicating that the reduced catalytic ability was not due to the stabilities of these NPs. The reduced catalytic activities are likely due to the adsorption of the yielded 4-aminophenol onto the surface of noble metals, which blocks the reactants from approaching the metal surface and results in a reduction in catalytic activity.[15]

CONCLUSION

In summary, mesoporous SnO_2-coated AuNSs, AuNRs, and Au/AgNRs have been prepared to study their applications in molecular sensing and catalysis. These core−shell NPs exhibited significantly improved stability in various organic solvents. The mesoporous nature of the SnO_2 shell was confirmed by the obvious redshift of LSPR band of these SnO_2 coated metal NPs with the increasing refractive index of the medium. High refractive index sensitivity of Au/AgNR/SnO_2 makes them promising materials for LSPR based molecular sensing. The mesoporous SnO_2 shell allows the metal core to be directly exposed to the surrounding environment to maintain their catalytic activity. The catalytic activities of these core−shell NPs for reduction of 4-nitrophenol was found to be dramatically enhanced compared to uncoated metal NPs. SnO_2-coated AuNR and Au/AgNR were found to display much better catalytic efficiency than SnO_2 coated AuNS. The enhanced catalytic activity of metal NPs upon SnO_2 coating was attributed to charge redistribution between noble metal and SnO_2 that helps to disperse electrons to a large area and prolonged electron lifetime in SnO_2 coated Au NPs, which facilitate the reduction of 4-nitrophenol. The charge transfer mechanism of enhanced catalytic efficiency of coated metal nanoparticles has been further demonstrated by photochemical reduction of silver ions on the outer surface of these NPs.

ASSOCIATED CONTENT

Supporting Information

Detailed preparation procedures of metal NPs; low-magnification and size distributions of SnO_2-coated metal NPs; XRD pattern and high-resolution TEM images of metal/SnO_2 NPs; Stability test of SnO_2-coated AuNRs; UV−vis absorption spectra of 4-nitrophenol before and after addition of AuNR/SnO_2 in the absence and presence of $NaBH_4$; plots of $\ln(C/C_0)$ versus reaction time for various catalytic reduction of 4-nitrophenolate by $NaBH_4$; TEM image of AuNR/SnO_2-10 nm and its catalytic data; TEM images of SnO_2 NPs and AuNS/SiO_2; recyclability test results; TEM images of SnO_2 coated metal NPs after catalytic reactions. This material is available free of charge via the Internet at http://pubs.acs.org.

AUTHOR INFORMATION

Corresponding Author

*E-mail: chmxqh@nus.edu.sg.

Notes

The authors declare no competing financial interest.

ACKNOWLEDGMENTS

This work is supported by the NUS AcRF Tier 1 grant (R-143-000-533-112), the Competitive Research Program (R-398-001-062-281) under National Research Foundation, and the SPORE program (COY-15-EWI-RCFSA/N197-1) under National Research Foundation and the Economic Development Board of Singapore.

REFERENCES

(1) Zeng, J.; Huang, J. L.; Lu, W.; Wang, X. P.; Wang, B.; Zhang, S. Y.; Hou, J. G. Necklace-like Noble-Metal Hollow Nanoparticle Chains: Synthesis and Tunable Optical Properties. *Adv. Mater.* **2007**, *19*, 2172−2176.

(2) Ghosh, S. K.; Pal, T. Interparticle Coupling Effect on the Surface Plasmon Resonance of Gold Nanoparticles: From Theory to Applications. *Chem. Rev.* **2007**, *107*, 4797−4862.

(3) Chen, H. J.; Ming, T.; Zhao, L.; Wang, F.; Sun, L. D.; Wang, J. F.; Yan, C. H. Plasmon-Molecule Interactions. *Nano Today* **2010**, *5*, 494−505.

(4) Willets, K. A.; Van Duyne, R. P. Localized Surface Plasmon Resonance Spectroscopy and Sensing. *Annu. Rev. Phys. Chem.* **2007**, *58*, 267−297.

(5) Anker, J. N.; Hall, W. P.; Lyandres, O.; Shah, N. C.; Zhao, J.; Van Duyne, R. P. Biosensing with Plasmonic Nanosensors. *Nat. Mater.* **2008**, *7*, 442−453.

(6) Mayer, K. M.; Hafner, J. H. Localized Surface Plasmon Resonance Sensors. *Chem. Rev.* **2011**, *111*, 3828−3857.

(7) Dotzauer, D. M.; Dai, J. H.; Sun, L.; Bruening, M. L. Catalytic Membranes Prepared using Layer-by-Layer Adsorption of Polyelectrolyte/Metal Nanoparticle Films in Porous Supports. *Nano Lett.* **2006**, *6*, 2268−2272.

(8) Park, J.; Huang, J.; Wang, W.; Murphy, C. J.; Cahill, D. G. Heat Transport between Au Nanorods, Surrounding Liquids, and Solid Supports. *J. Phys. Chem. C* **2012**, *116*, 26335−26341.

(9) Zhao, T.; Jiang, X. F.; Gao, N.; Li, S.; Zhou, N.; Ma, R.; Xu, Q. H. Solvent-Dependent Two-Photon Photoluminescence and Excitation Dynamics of Gold Nanorods. *J. Phys. Chem. B* **2013**, *117*, 15576−15583.

(10) Ai, L. H.; Yue, H. T.; Jiang, J. Environmentally Friendly Light-driven Synthesis of Ag Nanoparticles in Situ Grown on Magnetically Separable Biohydrogels as Highly Active and Recyclable Catalysts for 4-Nitrophenol Reduction. *J. Mater. Chem.* **2012**, *22*, 23447−23453.

(11) Jiang, C.; Guan, Z.; Rachel Lim, S. Y.; Polavarapu, L.; Xu, Q. H. Two-photon Ratiometric Sensing of Hg^{2+} by Using Cysteine Functionalized Ag Nanoparticles. *Nanoscale* **2011**, *3*, 3316−3320.

(12) Nam, J.; Won, N.; Jin, H.; Chung, H.; Kim, S. pH-Induced Aggregation of Gold Nanoparticles for Photothermal Cancer Therapy. *J. Am. Chem. Soc.* **2009**, *131*, 13639−13645.

(13) Jin, Z.; Xiao, M. D.; Bao, Z. H.; Wang, P.; Wang, J. F. A General Approach to Mesoporous Metal Oxide Microspheres Loaded with Noble Metal Nanoparticles. *Angew. Chem., Int. Ed.* **2012**, *51*, 6406−6410.

(14) Ai, L. H.; Zeng, C. M.; Wang, Q. M. One-step Solvothermal Synthesis of Ag-Fe_3O_4 Composite as a Magnetically Recyclable Catalyst for Reduction of Rhodamine B. *Catal. Commun.* **2011**, *14*, 68−73.

(15) Seh, Z. W.; Liu, S. H.; Zhang, S. Y.; Shah, K. W.; Han, M. Y. Synthesis and Multiple Reuse of Eccentric Au@TiO_2 Nanostructures as Catalysts. *Chem. Commun.* **2011**, *47*, 6689−6691.

(16) You, L.; Mao, Y. W.; Ge, J. P. Synthesis of Stable SiO_2@Au-Nanoring Colloids as Recyclable Catalysts: Galvanic Replacement

DOI: 10.1021/am508803c
ACS Appl. Mater. Interfaces 2015, 7, 4844−4850

Taking Place on the Surface. *J. Phys. Chem. C* **2012**, *116*, 10753−10759.
(17) Li, H. Q.; Han, L. N.; Cooper-White, J.; Kim, I. Palladium Nanoparticles Decorated Carbon Nanotubes: Facile Synthesis and Their Applications as Highly Efficient Catalysts for the Reduction of 4-Nitrophenol. *Green Chem.* **2012**, *14*, 586−591.
(18) Mei, Y.; Lu, Y.; Polzer, F.; Ballauff, M.; Drechsler, M. Catalytic Activity of Palladium Nanoparticles Encapsulated in Spherical Polyelectrolyte Brushes and Core-Shell Microgels. *Chem. Mater.* **2007**, *19*, 1062−1069.
(19) Zhao, T. T.; Wu, H.; Yao, S. Q.; Xu, Q. H.; Xu, G. Q. Nanocomposites Containing Gold Nanorods and Porphyrin-Doped Mesoporous Silica with Dual Capability of Two-Photon Imaging and Photosensitization. *Langmuir* **2010**, *26*, 14937−14942.
(20) Chang, Y. T.; Liao, P. Y.; Sheu, H. S.; Tseng, Y. J.; Cheng, F. Y.; Yeh, C. S. Near-Infrared Light-Responsive Intracellular Drug and siRNA Release Using Au Nanoensembles with Oligonucleotide-Capped Silica Shell. *Adv. Mater.* **2012**, *24*, 3309−3314.
(21) Lee, J.; Park, J. C.; Song, H. A Nanoreactor Framework of a Au@SiO_2 Yolk/Shell Structure for Catalytic Reduction of p-Nitrophenol. *Adv. Mater.* **2008**, *20*, 1523−1528.
(22) Wu, C. L.; Xu, Q. H. Stable and Functionable Mesoporous Silica-Coated Gold Nanorods as Sensitive Localized Surface Plasmon Resonance (LSPR) Nanosensors. *Langmuir* **2009**, *25*, 9441−9446.
(23) Wang, D. W.; Tejerina, B.; Lagzi, I.; Kowalczyk, B.; Grzybowski, B. A. Bridging Interactions and Selective Nanoparticle Aggregation Mediated by Monovalent Cations. *ACS Nano* **2011**, *5*, 530−536.
(24) Oldfield, G.; Ung, T.; Mulvaney, P. Au@SnO_2 Core−Shell Nanocapacitors. *Adv. Mater.* **2000**, *12*, 1519−1522.
(25) Yu, K.; Wu, Z. C.; Zhao, Q. R.; Li, B. X.; Xie, Y. High-Temperature-Stable Au@SnO_2 Core/Shell Supported Catalyst for CO Oxidation. *J. Phys. Chem. C* **2008**, *112*, 2244−2247.
(26) Lee, S. H.; Rusakova, I.; Hoffman, D. M.; Jacobson, A. J.; Lee, T. R. Monodisperse SnO_2-Coated Gold Nanoparticles are Markedly More Stable than Analogous SiO_2-Coated Gold Nanoparticles. *ACS Appl. Mater. Interfaces* **2013**, *5*, 2479−2484.
(27) Chen, H.; Shao, L.; Li, Q.; Wang, J. Gold Nanorods and Their Plasmonic Properties. *Chem. Soc. Rev.* **2013**, *42*, 2679−2724.
(28) Yu, K.; Polavarapu, L.; Xu, Q. H. Excitation Wavelength and Fluence Dependent Femtosecond Transient Absorption Studies on Electron Dynamics of Gold Nanorods. *J. Phys. Chem. A* **2011**, *115*, 3820−3826.
(29) Nikoobakht, B.; El-Sayed, M. A. Preparation and Growth Mechanism of Gold Nanorods (NRs) using Seed-Mediated Growth Method. *Chem. Mater.* **2003**, *15*, 1957−1962.
(30) Huang, Y. J.; Kim, D. H. Synthesis and Self-Assembly of Highly Monodispersed Quasispherical Gold Nanoparticles. *Langmuir* **2011**, *27*, 13861−13867.
(31) Okuno, Y.; Nishioka, K.; Kiya, A.; Nakashima, N.; Ishibashi, A.; Niidome, Y. Uniform and Controllable Preparation of Au-Ag core-shell Nanorods using Anisotropic Silver Shell Formation on Gold Nanorods. *Nanoscale* **2010**, *2*, 1489−1493.
(32) Tripathy, S. K.; Kwon, H. W.; Leern, Y. M.; Kim, B. G.; Yu, Y. T. Ag@SnO_2 Core-Shell Structure Nanocomposites. *Chem. Phys. Lett.* **2007**, *442*, 101−104.
(33) Lee, Y. H.; Chen, H.; Xu, Q. H.; Wang, J. Refractive Index Sensitivities of Noble Metal Nanocrystals: The Effects of Multipolar Plasmon Resonances and the Metal Type. *J. Phys. Chem. C* **2011**, *115*, 7997−8004.
(34) McFarland, A. D.; Van Duyne, R. P. Single Silver Nanoparticles as Real-Time Optical Sensors with Zeptomole Sensitivity. *Nano Lett.* **2003**, *3*, 1057−1062.
(35) Charles, D. E.; Aherne, D.; Gara, M.; Ledwith, D. M.; Gun'ko, Y. K.; Kelly, J. M.; Blau, W. J.; Brennan-Fournet, M. E. Versatile Solution Phase Triangular Silver Nanoplates for Highly Sensitive Plasmon Resonance Sensing. *ACS Nano* **2009**, *4*, 55−64.
(36) Chen, H.; Kou, X.; Yang, Z.; Ni, W.; Wang, J. Shape- and Size-Dependent Refractive Index Sensitivity of Gold Nanoparticles. *Langmuir* **2008**, *24*, 5233−5237.
(37) Jana, N. R.; Gearheart, L.; Murphy, C. J. Wet Chemical Synthesis of Silver Nanorods and Nanowires of Controllable Aspect Ratio. *Chem. Commun.* **2001**, 617−618.
(38) Zhang, P.; Shao, C. L.; Zhang, Z. Y.; Zhang, M. Y.; Mu, J. B.; Guo, Z. C.; Liu, Y. C. In Situ Assembly of Well-Dispersed Ag Nanoparticles (AgNPs) on Electrospun Carbon Nanofibers (CNFs) for Catalytic Reduction of 4-Nitrophenol. *Nanoscale* **2011**, *3*, 3357−3363.
(39) Zhang, P. H.; Sui, Y. M.; Xiao, G. J.; Wang, Y. N.; Wang, C. Z.; Liu, B. B.; Zou, G. T.; Zou, B. Facile Fabrication of Faceted Copper Nanocrystals with High Catalytic Activity for p-Nitrophenol Reduction. *J. Mater. Chem. A* **2013**, *1*, 1632−1638.
(40) Zeng, J.; Zhang, Q.; Chen, J. Y.; Xia, Y. N. A Comparison Study of the Catalytic Properties of Au-Based Nanocages, Nanoboxes, and Nanoparticles. *Nano Lett.* **2010**, *10*, 30−35.
(41) Deng, Y. H.; Cai, Y.; Sun, Z. K.; Liu, J.; Liu, C.; Wei, J.; Li, W.; Liu, C.; Wang, Y.; Zhao, D. Y. Multifunctional Mesoporous Composite Microspheres with Well-Designed Nanostructure: A Highly Integrated Catalyst System. *J. Am. Chem. Soc.* **2010**, *132*, 8466−8473.
(42) Guo, X.; Zhang, Q.; Sun, Y. H.; Zhao, Q.; Yang, J. Lateral Etching of Core-Shell Au@Metal Nanorods to Metal-Tipped Au Nanorods with Improved Catalytic Activity. *ACS Nano* **2012**, *6*, 1165−1175.
(43) Bonacic-Koutecky, V.; Burda, J.; Mitric, R.; Ge, M. F.; Zampella, G.; Fantucci, P. Density Functional Study of Structural and Electronic Properties of Bimetallic Silver-Gold Clusters: Comparison with Pure Gold and Silver Clusters. *J. Chem. Phys.* **2002**, *117*, 3120−3131.
(44) Seh, Z. W.; Liu, S. H.; Zhang, S. Y.; Bharathi, M. S.; Ramanarayan, H.; Low, M.; Shah, K. W.; Zhang, Y. W.; Han, M. Y. Anisotropic Growth of Titania onto Various Gold Nanostructures: Synthesis, Theoretical Understanding, and Optimization for Catalysis. *Angew. Chem., Int. Ed.* **2011**, *50*, 10140−10143.
(45) Zhu, C. Z.; Wang, P.; Wang, L.; Han, L.; Dong, S. J. Facile Synthesis of Two-Dimensional Graphene/SnO_2/Pt Ternary Hybrid Nanomaterials and Their Catalytic Properties. *Nanoscale* **2011**, *3*, 4376−4382.
(46) Zhou, N.; Polavarapu, L.; Gao, N.; Pan, Y.; Yuan, P.; Wang, Q.; Xu, Q. H. TiO_2 Coated Au/Ag Nanorods with Enhanced Photocatalytic Activity under Visible Light Irradiation. *Nanoscale* **2013**, *5*, 4236−4241.
(47) Linic, S.; Christopher, P.; Ingram, D. B. Plasmonic-Metal Nanostructures for Efficient Conversion of Solar to Chemical Energy. *Nat. Mater.* **2011**, *10*, 911−921.
(48) Seh, Z. W.; Liu, S.; Low, M.; Zhang, S.-Y.; Liu, Z.; Mlayah, A.; Han, M.-Y. Janus Au-TiO_2 Photocatalysts with Strong Localization of Plasmonic Near-Fields for Efficient Visible-Light Hydrogen Generation. *Adv. Mater.* **2012**, *24*, 2310−2314.

DOI: 10.1021/am508803c
ACS Appl. Mater. Interfaces 2015, 7, 4844−4850